Combined hemicellulolytic and phenoloxidase activities of Thermobacillus xylanilyticus enable growth on lignin-rich substrates and the release of phenolic molecules

Quentin Czerwiec, Brigitte Chabbert, David Crônier, Bernard Kurek, Harivony Rakotoarivonina

Bioresource Technology 397 (2024) 130507

Contents lists available at ScienceDirect

Bioresource Technology

journal homepage: www.elsevier.com/locate/biortech

Combined hemicellulolytic and phenoloxidase activities of *Thermobacillus xylanilyticus* enable growth on lignin-rich substrates and the release of phenolic molecules

Quentin Czerwiec [a,b,1], Brigitte Chabbert [a], David Crônier [a], Bernard Kurek [a], Harivony Rakotoarivonina [a,b,*]

[a] Université de Reims Champagne-Ardenne, INRAE, FARE, UMR A 614, Reims, France
[b] Université de Reims Champagne-Ardenne, INRAE, FARE, UMR A 614, AFERE, Reims, France

HIGHLIGHTS

- *T. xylanilyticus* grows on lignin-rich substrates as kraft lignin and steam exploded wheat straw.
- Oxidoreductases and hemicellulases are expressed differently depending on the substrate.
- Oxidoreductases are likely involved in detoxification process in cultures with lignins.
- Despite few lignin structural modifications phenolic compounds are released in the culture media.

GRAPHICAL ABSTRACT

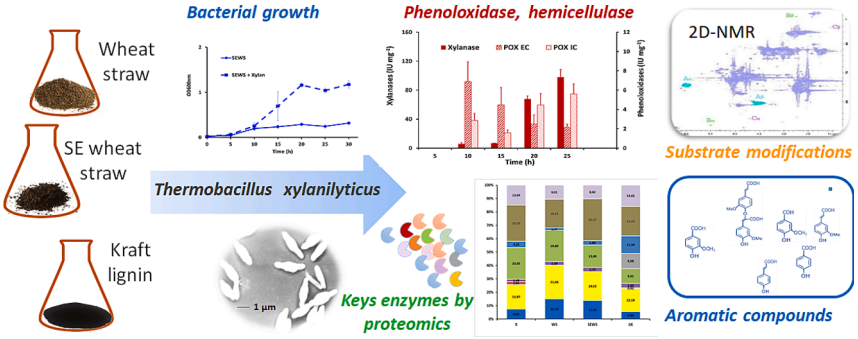

ARTICLE INFO

Keywords:
Phenolic compounds
Lignocellulolytic enzymes
Kraft lignin
Bacteria
Detoxifications

ABSTRACT

Major challenge in biorefineries is the use of all lignocellulosic components, particularly lignins. In this study, *Thermobacillus xylanilyliticus* grew on kraft lignin, steam-exploded and native wheat straws produced different sets of phenoloxidases and xylanases, according to the substrate. After growth, limited lignin structural modifications, mainly accompanied by a decrease in phenolic acids was observed by Nuclear Magnetic Resonance spectroscopy. The depletion of *p*-coumaric acid, vanillin and *p*-hydroxybenzaldehyde combined to vanillin production in the culture media indicated that the bacterium can transform some phenolic compounds. Proteomic approaches allowed the identification of 29 to 33 different hemicellulases according to the substrates. Twenty oxidoreductases were differentially expressed between kraft lignin and steam-exploded wheat straw. These oxidoreductases may be involved in lignin and aromatic compound utilization and detoxification. This study highlights the potential value of *Thermobacillus xylanilyticus* and its enzymes in the simultaneous valorization of hemicellulose and phenolic compounds from lignocelluloses.

* Corresponding author.
E-mail addresses: czerwiec@casf-bischwiller.net (Q. Czerwiec), brigitte.chabbert@inrae.fr (B. Chabbert), david.cronier@inrae.fr (D. Crônier), bernard.kurek@inrae.fr (B. Kurek), harivony.rakotoarivonina@univ-reims.fr (H. Rakotoarivonina).
[1] Present address : Savoirs Vivants, Haguenau, France

https://doi.org/10.1016/j.biortech.2024.130507
Received 26 September 2023; Received in revised form 26 February 2024; Accepted 26 February 2024
Available online 28 February 2024

1. Introduction

Lignocelluloses are renewable resources issued from agriculture, forest and their related industries. They can be converted into energy, molecules and materials, by various technologies, contributing therefore to the mobilization and cycling of renewable carbon in non-food applications. They are constituted by a complex arrangement of cellulose, hemicellulose and lignins. Lignocelluloses structure depend on their origin and on the various technological transformations they have undergone. Cellulose and hemicellulose, are used to produce energy, biofuels and high-value-added molecules (Nargotra et al., 2023). Lignin is the first source of renewable aromatic compounds on earth, with great potential for fine chemical, bio-oils and resins (Sethupathy et al., 2022). It is a complex aromatic and phenolic structure with high heterogeneity, from molecular to polymeric scale. It is partly responsible for the recalcitrance to conversion of lignin-rich substrates by limiting access of reactants to polysaccharides, and by hindering enzyme activities through hydrophobic interactions for instance (McCann and Carpita, 2015). However, to design a sustainable environmental and economical biorefinery for lignocelluloses, the valorization of all the components of lignin-rich substrates are requested. A major unsolved and actual challenge is the rational removal of lignin and its conversion into valuable components. Currently, at the industrial level, there is no economically viable recovery route for aromatic molecules derived from lignin despite promising demonstrations (Moretti et al., 2021). Lignins remain underused and are mainly burned to provide heat and energy. Among several options, the biological conversion of lignin, due to its specificity and low environmental impact, is suggested as an ideal approach for enhancing lignin conversion, complementing the panel of physico-chemical degradation. These later usually requires harsh conditions high energy input, and generating uncontrolled sets of unwanted by products. Many studies have been focused on the ability of fungi and their enzymes to use and convert lignin or derived aromatic compounds into valuable products. Fungal lignin transformations occur through a set of extracellular lignin-modifying enzymes (laccases and peroxidases) and lignin auxiliary enzymes (da Silva Vilar et al., 2022). Although less documented in the 1980–2010 period, bacteria are also known to use and mineralize lignins and lignin derivatives through a set of metabolic pathways including numerous oxidoreductases (Bugg et al., 2020). Bacteria belonging to the *Betaproteobacteria* (*Sphingomonas*, *Sphingobium*, *Pseudomonas*, etc.) and *Actinobacteria* (*Rhodococcus*, *Streptomyces*, etc.) phyla are known to be the major lignin-derived aromatic degraders. Alternatively, they are able to use lignin as carbon source and to produce high-value-added products, by natural routes or after strain improvement by metabolic engineering (Bugg et al., 2020). Understanding the behaviour of microorganisms in the presence of lignin-rich substrates with different compositions will improve biorefinery of lignocellulosic biomasses, including the lignin fractions. Furthermore, the knowledge-based approach will also facilitate the discovery of efficient biocatalysts in lignin utilisation. Among candidates for biotechnological lignocellulose biorefinery, *Thermobacillus xylanilyticus* (*TX*) is a thermophilic bacterium that produces hemicellulolytic enzymes, including endoxylanases, arabinofuranosidases and feruloyl esterases. *TX* modulates its hemicellulases production according to the composition of the lignocelluloses used as a carbon source (Rakotoarivonina et al., 2014). Recently, the genome of this bacterium was sequenced; many hemicellulases have been identified, and oxidoreductases encoding genes have been annotated. Some of these genes encode peroxidases, laccases, putative H_2O_2-producing enzymes and putative enzymes involved in the intracellular metabolism of aromatic compounds (Rakotoarivonina et al., 2022). These enzymes are known for their involvement in lignin and lignin derivatives utilization or conversion in many ligninolytic bacteria (Bugg et al., 2020). Thus, the genomic data of *TX* suggest possible links between the degradation of hemicelluloses and the use of lignin and related components. *TX* can be considered as an interesting biological tool for studying these interactions within bacteria; it subsequently opens the way toward the simultaneous valorization of both substrates. The present study aimed to understand the functioning of *TX* in the presence of representative lignin-rich substrates: native wheat straw (WS); biorefinery residues resulting from pre-treatments (steam exploded wheat straw (SEWS)) and industrial technical kraft lignin (KL). The issue is to delineate the relation between *TX* growths on the complex substrates and their modification, the enzymatic activities productions and the expression of its genomic potential by multiple complementary approaches. Bacterial growth was followed, and phenoloxidase and xylanase activities productions were monitored. Proteomic approach was used to identify key proteins that are activated by the bacterium on the different substrates. Finally, changes in the phenolic compound composition in the culture media and the structure of the lignin-rich substrates were studied after bacterial growth to highlight and qualify the extent of modification of lignins and lignocellulose components.

2. Materials and methods

2.1. Bacterial strain, growth, and culture conditions

T. xylanilyticus strain was obtained from the Collection Nationale de Cultures de Microorganismes (France) under the number CNCM I-1017. The bacterium was cultivated on basal media supplemented with 10 % CO_2. WS (ARD, Pomacle, France), SEWS (IFPEN, Solaize, France) and KL (Sigma Aldrich, France) were used as carbone source alone at 5 g/L, or used supplemented with 2.5 g/L of beechwood xylan (Roth, Germany). The culture conditions and preparations were described by (Rakotoarivonina et al., 2014). All cultures were performed in triplicate.

2.2. Kinetic growth, protein preparation and activities

Growth was followed during 30 h by measuring every 5 h the optical density at 600 nm ($OD_{600\ nm}$) of culture diluted or not. Maximal growth rate (μ_{max}) was determined during exponential growth. The supernatant (extracellular proteins EC) were recovered after centrifuging the cultures for 10 min at 5500 rpm without residual particles. The cell pellet was suspended in 1 mL of 25 mM Tris-HCl buffer at pH 7 and were broken mechanically using a FastPrep-24TM 5G (MP Biomedicals, France) homogenizer. The lysates were centrifuged at 8000 rpm for 5 min; the supernatant corresponded to the IC proteins. A protein assay was performed with Bradford reagent (Sigma Aldrich, France) according to the manufacturer's recommendations. Xylanase activities were determined by measuring the reducing sugars released from xylan by spectrophotometry and using 0.5 % w/v beechwood xylan solubilized in 25 mM Tris-HCl buffer at pH 7 and 100 µl of IC or EC proteins as previously described (Rakotoarivonina et al., 2014). Phenoloxidase (POX) activity was measured using pyrogallol at 50 °C for 5 min. The activities were determined by spectrophotometric quantification of purpurogallin derived from pyrogallol oxidation. The assay mixture contained 25 mM Tris-HCl buffer at pH 7, 8 mM pyrogallol, 1 mM EDTA, 0.5 mM H_2O_2 final concentration and 100 µl of EC or IC samples. POX activities were calculated by using the molar extinction coefficient of the purpurogallin at 420 nm of 2.21 $mM^{-1}\ cm^{-1}$. The activities are expressed as IU per mg of EC or IC proteins. One IU xylanase or POX activity corresponded to 1 µmol of xylose or purpurogallin respectively liberated per min.

Culture media containing the same carbon sources but without bacterial inoculation incubated and sampled regularly were used as blanks for the different analyses.

2.3. Identification of key enzymes by proteomics

For proteomics, 50 mL of each *TX* culture was grown in triplicate. After 25 h of growth on the different substrates, the IC and EC proteins were recovered as described above, except the IC proteins were 10-fold concentrated. Proteins (10 µg) were separated by SDS–PAGE (sodium

dodecyl sulphate–polyacrylamide gel electrophoresis) and stained using colloidal Coomassie blue, before proteomic analyses, performed at the Metabolomic and Proteomic Exploration Facility (INRAE, Saint-Genès Champanelle, France). After trypsin hydrolysis, the peptides were analysed via nano-LC–MS/MS using an Ultimate 3000 system coupled to an LTQ Orbitrap Velos mass spectrometer (Thermo ScientificTM) with a nanoelectrospray ionization source and protocols usually used on the platform.

For protein identification, an MS/MS ion search was performed with Mascot v2.5 (http://www.matrixscience.com) against the local *T. xylanilyticus* database (3956 sequences, version fasta file). Protein was validated when at least two peptides originating from one protein showed statistically significant identity above Mascot scores > 16 with a false discovery rate of 3 % (significance threshold $p < 0.05$). Protein identification was performed using Proteome Discoverer 1.4 software (ThermoElectron). This analysis provided protein abundance information as described previously (Ishihama et al., 2005).

Label-free protein quantification analysis, which quantifies the level of expression of different proteomes studied, was performed with Progenesis QI (Nonlinear Dynamics, Waters, USA), with a control condition (xylan). The profile data of the MS scans and MS/MS scans provided positional information (*m/z* and retention time) and peptide abundance. All unique validated peptides of an identified protein were included, and the total cumulative abundance was calculated by summing the abundances of all peptides allocated to the respective protein.

2.4. Genome annotations for functional assignation

To identify proteins involved in various pathways, the 3956 protein sequences from the genome of *TX* annotated previously (Rakotoarivonina et al., 2022); draft genome available at https://www.ebi.ac.uk/ena/browser/home; study accession number PRJEB43105; were compared to pathways references in Kyoto encyclopedia of genes and genomes (KEGG database) using KAAS server (KEGG automatic annotation server) at http://www.genome.jp/kegg/kaas/. KEGG orthology (KO), EC numbers of enzymes and proteins involved in different pathways were obtained. Protein sequence analyses (with oxidoreductases of interest) were performed by Blast using facilities at https://papers.genomics.lbl.gov, to find the best hits with characterized proteins. Sequence similarity searches with non-redundant database with Uniport database were performed with the facilities at https//https://www.uniprot.org/blast.

2.5. Chemical composition of the lignin-rich substrates

Chemical analyses of the lignin-rich substrates were performed in triplicate on dry samples. Sugar analysis was carried out by high-performance anion-exchange chromatography (HPAEC) after acid hydrolysis of the substrates (Auxenfans et al., 2017). The lignin content was determined at 280 nm after solubilization of the samples with acetyl bromide in acidic medium (Iiyama K, 1988). The lignin content was calculated using the extinction coefficient of grass lignin (20 l g^{-1} cm^{-1}). Ester-bound, and ether-bound phenolic acids were released by alkaline hydrolyses (2 M NaOH at 35 °C and 4 M NaOH at 170 °C) as described by Auxenfans et al. (2017). The recovered alkaline filtrate was acidified to pH 1 with 6 M HCl, mixed with 3,4,5-trimethoxy-*trans*-cinnamic acid as an internal standard and extracted three times with 25 mL of diethyl ether. Phenolic acids were quantified at 302 nm and 280 nm by high-performance liquid chromatography (HPLC) as described by Auxenfans et al. (2017) on a Spherisorb S5-0DS2, RP18, 4.6 × 250 mm column equipped with a photodiode array detector (Waters, USA). The ether-bound phenolic acid content was determined by evaluating the difference between the total and esterified phenolic acid contents.

2.6. Analysis of the phenolic compounds in the culture media

The content of phenolic compounds in the controls and inoculated culture media was determined by HPLC after 25 h incubation as described above (Section 2.4), except that phenolic compounds were directly extracted with diethyl ether from 5 mL of culture media after acidification to pH 1 with 6 M HCl.

2.7. Spectroscopic and nuclear magnetic resonance analyses of lignin-rich residues

WS and SEWS recovered after 25 h incubation with or without bacteria were washed three times with distilled water and dried at 45 °C for 24 h before being stored at 4 °C until use. For KL, 5 mL of culture media supernatant free of bacteria, or controls KL media were frozen at −20 °C and freeze-dried. Transmission FTIR spectra were obtained for 2 mg of residue mixed with KBr (120 mg) using a Nicolet 6700 (Thermo Fisher Scientist, USA). Spectra were obtained from 16 scans performed between 400 and 4000 cm^{-1} with a spectral resolution of 4 cm^{-1}. All infrared spectra in the 2000–800 cm^{-1} region were baseline corrected and normalized by fixing the area under the spectrum using Unscrambler® X (Camo Analytics) software.

Before liquid phase 2D HSQC NMR characterization, samples were ultra-milled and 100 mg were acetylated in a mixture of DMSO/N-methylimidazole and then in acetic acid (Mansfield et al., 2012). Acetylated samples were washed then dried prior to solubilization in deuterated chloroform for NMR analysis in a 5 mm NMR tube. Spectra acquisition was performed by a 600 MHz Bruker Biospin Avance III spectrometer (Bruker, Germany) using a 5 mm TCI cryoprobe and equipped with TopSpin 3.1 software as described previously (Auxenfans et al., 2017). The 2D profiles were calibrated on CDCl3: ^{1}H: 7.26 ppm; ^{13}C: 77.2 ppm. Peaks were assigned according to literature data (Mansfield et al., 2012). Spectra were normalized to the amount of unit G on carbon 2.

2.8. Statistical analysis

One-way analysis of variance was performed to compare growth rate, enzymatic activities, and phenolic compounds from the triplicate cultivations according to growth conditions or culture durations using SigmaPlot® software (version 12.0, Systat, USA). The Holm–Sidak method was used to perform pairwise multiple comparisons, with a p value < 0.05 indicating a significant difference. Statistical analysis of the proteomic data was performed using the "between subject design", and comparisons were made using one-way analysis of variance (ANOVA) for the different conditions with Progenesis QI software (Non linear Dynamics, Waters, USA). The expression of a protein was considered to be significantly different if the q value was < 0.05 (p < 0.05 adjusted with a false discovery rate (FDR) < 0.05).

3. Results and discussion

3.1. Substrate composition

Chemical analyses indicated that WS, SEWS, and KL have different polysaccharide and lignin contents (Table 1). The sugar composition of WS (58 % DM), which consists mainly of glucose (34 % DM), xylose (21 % DM) and arabinose (3 % DM), corresponds to that of typical grass cell walls (Scheller and Ulvskov, 2010). After steam explosion, the SEWS polysaccharides (54 % DM) were mostly composed of glucose, and the low content of xylose agrees with the removal of hemicelluloses from lignocellulosic biomasses via steam explosion (Auxenfans et al., 2017). KL was almost entirely composed of lignin (85 % DM), with trace amount of sugars, whereas SEWS and WS had lower lignin contents (30 and 24 % DM, respectively). WS and SEWS contained both esterified and etherified phenolic acids (*p*-coumaric acid, ferulic acid and β-O-4

Table 1
Chemical composition of the lignin-rich substrates.

	WS	SEWS	KL
Glucose	34.2 ± 0.5	48.0 ± 0.5	0.1 ± 0.0
Xylose	20.6 ± 0.2	5.8 ± 0.0	0.3 ± 0.0
Arabinose	2.9 ± 0.1	0.4 ± 0.0	0.2 ± 0.0
Lignin	23.7 ± 2.0	30.3 ± 0.9	85.3 ± 1.0
p-coumaric acid			
Ester	3261.6 ± 13.5	2878.3 ± 74.5	/
Ether	2508.0 ± 104.6	2964.8 ± 169.5	/
Ferulic acid			
Ester	1843.5 ± 36.0	1300.2 ± 91.5	/
Ether	3397.1 ± 32.2	1559.5 ± 27.6	/
Di-ferulic acid (β-O-4)			
Ester	/	/	/
Ether	281.0 ± 17.1	287.7 ± 12.9	/

Glucose, xylose, arabinose and lignin (as % w/w dry matter); *p*-coumaric, ferulic and di-ferulic acids (as μg g^{-1} dry matter).
/= Undetected.

diferulic acid). These acids are covalently bound to hemicelluloses and lignin in grass cell walls (Ralph, 2010). Such interpolymer interactions can play a negative role in the accessibility of lignocellulosic cell walls to microorganisms and enzymes (McCann and Carpita, 2015). Overall, the chemical data confirmed that the selected lignin-rich substrates have contrasting lignin and sugars content and compositions. Thus, the availability of sugars may be different depending on their distribution and possible interactions within the biomass matrix (McCann and Carpita, 2015). It is then hypothesized that the various lignin-rich substrates, will heterogeneously impact the physiology of *TX* through its ability to use them as carbon sources.

3.2. Bacterial growth and enzymatic activities

3.2.1. Cultivation of Thermobacillus xylanilyticus on lignin-rich substrates

TX was able to grow in the presence of all different lignin-rich substrates alone (KL, SEWS and WS) (Fig. 1A–C continuous line). Growth occurred after lag phases of 15 h on KL and 5 h on SEWS and WS. The growth of *TX* on the SEWS was significantly lower ($p < 0.001$) than that on the WS and KL cultures (μ_{max} of only 0.2 ± 0.0 h^{-1} *vs.* 0.5 ± 0.1 h^{-1} and 0.6 ± 0.1 h^{-1} for WS and KL, respectively). The bacteria maintained this low growth rate throughout the cultivation period. This study showed, for the first time, that *TX* can grow on KL alone and on a highly modified wheat straw (SEWS), indicating its ability to use some or all of their constitutive molecules as a carbon source. During growth on lignin-rich substrates as the sole carbon source, *TX* produced POX activities intracellularly and extracellularly (POX IC and POX EC) and xylanase whose levels varied according to the substrate (Fig. 1D–F). To the best of our knowledge, phenoloxidase activities were measured for the first time, in this hemicellulolytic bacterium.

In cultures with KL (Fig. 1D), POX IC activity was measured only during the growth phase, at a maximal level of 5 IU/mg, at which point the activity decreased significantly ($p < 0.001$) until the end of cultivation. The production of only POX IC suggested that *TX* could utilize some phenolic molecules potentially present in KL medium. Kraft lignin is polydisperse at the molecular weight level. Thus, the low-mass aromatic compounds can be internalized and stimulate the production of intracellular enzymes to allow their metabolization (Abdelaziz and Hulteberg, 2017). The decrease in the POX IC over time may be explained by the use of these molecules. The absence of EC activity suggested that, at this stage, the growth was decoupled from possible extracellular lignin degradation by the bacterium. No xylanase activity was detected, which is not surprising as KL contains very little sugar, and xylanase production is often induced by the presence of xylan or hemicellulose. Considering the absence of *TX* growth on basal media alone (see See Supplementary Material), the low growth of *TX* on KL media and the production of POX IC, one can hypothesize that *TX* can use the phenolic monomers present in the media and even some components of KL itself. Numerous studies have shown the ability of various bacteria to use KL and mono - or oligo-mers phenolic molecules derived from lignins as carbon sources (Kumar et al., 2018; Taylor et al., 2012). Recently, thermophilic *Geobacilli* were isolated from the environment by using purified lignin as the sole carbon source (Mesle et al., 2022). Noteworthy, the growth of *TX* on KL was similar to or higher than the growth of some ligninolytic bacteria, such as *Rhodococcus jostii* RHA and *Bacillus ligniniphilus* L1 on KL. (Sainsbury et al., 2013; Zhu et al., 2017).

Several studies have also reported the efficient growth of microorganisms on various steam-exploded lignocellulosic biomasses as sole carbon sources, but this growth is frequently observed in cocultures or consortia (Shi et al., 2019; Zhang et al., 2023). Here, *TX* alone was able to grow in the presence of SEWS but exhibited low and regular growth (Fig. 1B). This low growth may be explained by the structural changes in lignocellulosic substrates after steam explosion, which limit access to carbohydrate polymers (Ballesteros et al., 2006), and can induce the formation of bacterial growth inhibitors (Klinke et al., 2004). Likewise, despite the presence of sugars in SEWS, no xylanase activity was detected, suggesting that SEWS xylan is not available to support the observed low bacterial growth. On the SEWS, dynamic production of POX (EC and IC) activity was detected just after the lag phase of growth (10 h) (Fig. 1E). The maximum POX EC activity was obtained at the beginning of the exponential growth phase (8 IU/mg protein) and then decreased significantly ($p < 0.001$) over time. POX IC activity increased until it reached its maximum level (~3 IU.mg^{-1}) at the end of cultivation. Even if the use of certain soluble sugars in the medium cannot be excluded, the complexity of SEWS and the presence of lignin could induce the observed production of EC POX activities, followed by the activation of IC activities. These activities are necessary for the bacteria to either detoxify the medium or to attempt to use the lignin and to support the low growth and survival of the bacterium on SEWS. Generally, the conversion of lignin requires the production of EC oxidoreductases (peroxidases and laccases), after which IC oxidoreductases metabolize aromatic compounds *via* different intracellular pathways (da Silva Vilar et al., 2022, Bugg et al., 2020).

On WS (Fig. 1F), in accordance with previous studies on this bacterium (Rakotoarivonina et al., 2014), xylanase activity (80 ± 18 IU/mg at the end of the culture) was the main enzymatic activity produced. Along with xylanase activity, POX activities were concomitantly detected intracellularly and extracellularly. POX EC levels significantly ($p < 0.001$) decreased, whereas POX IC levels remained stable at approximately 4 UI.mg^{-1} during the culture. As reported for various ligninolytic and/or lignocellulolytic microorganisms, the production of hemicellulases and some ligninolytic enzymes is stimulated in the presence of lignocellulosic biomasses and lignin-rich substrates (Aston et al., 2016; Mardetko et al., 2021; Zhu et al., 2017).

3.2.2. Cultivation of Thermobacillus xylanilyticus on xylan-supplemented lignin-rich substrates

To highlight the interaction between bacterial use of hemicellulose and of lignin-rich substrate and to improve *TX* growths, xylan was added to the culture media. The presence of xylan increased *TX* growth under all the conditions (KL, SEWS and WS). The maximal OD_{600nm} values increased 3- and 4-fold for all substrates (Fig. 1A–C dotted lines) and enhanced the growth rate (20 % significant increase for WS and SEWS (*p* value < 0,001) and 9 % for KL). Accordingly, xylanase activities were detected regardless of the substrate (Fig. 1G–I). Overall, the highest xylanase activities were measured during the stationary phase. Xylan or small oligosaccharide substrates are known to stimulate the production of xylanases by lignocellulolytic microorganisms, which can then quickly degrade xylan, as previously shown for *TX* cultures with wheat bran, wheat straw or xylooligosaccharides (Rakotoarivonina et al., 2014). Generally, as bacterial lignin degradation is rather slow, growth on this substrate often requires an additional accessible carbon source (DeAngelis et al., 2013; Glaser and Venus, 2017; Ravi et al., 2019). In the

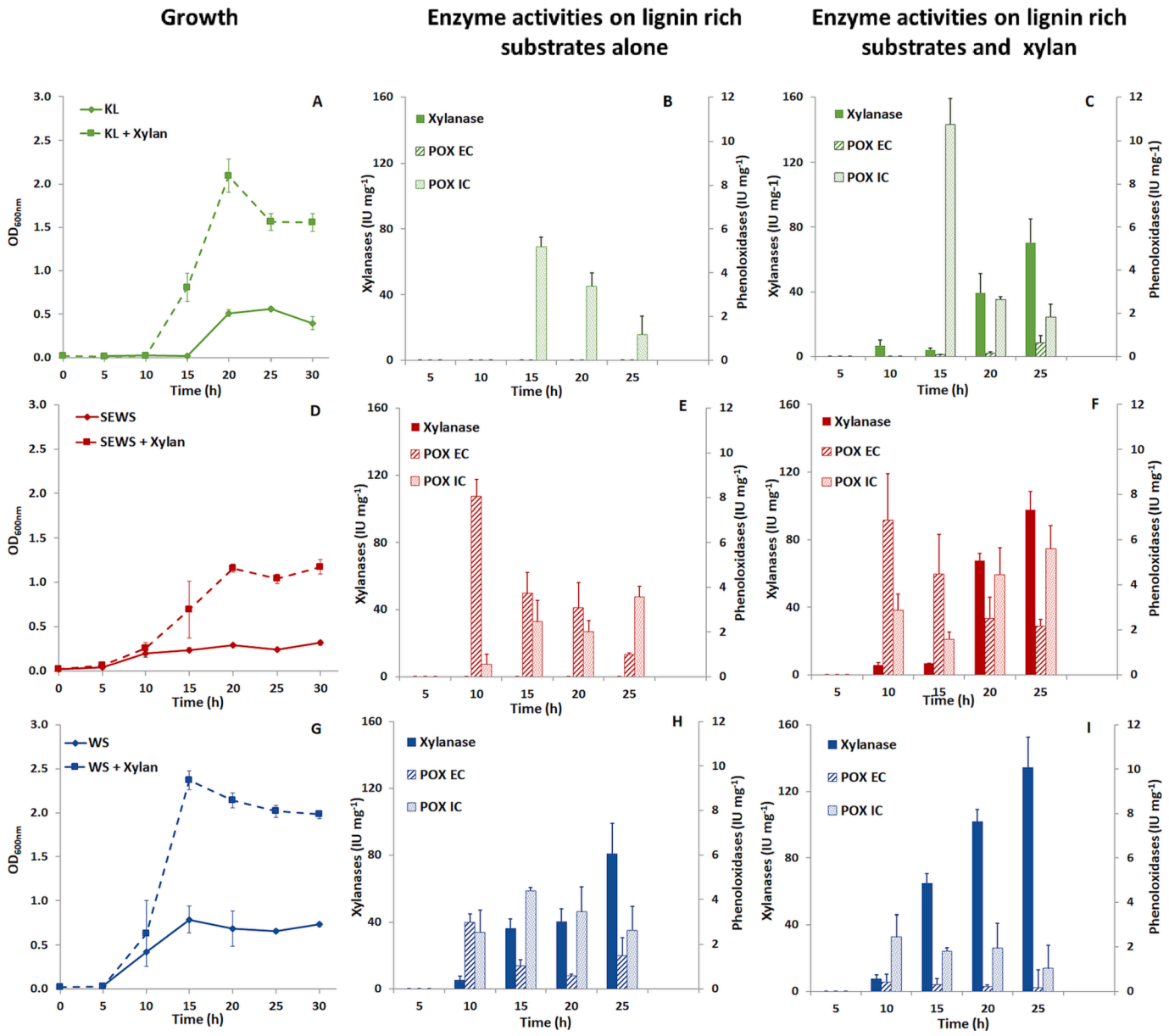

Fig. 1. Growth and phenoloxidase and xylanase activities detected in intracellular (IC) or extracellular (EC) cell compartments in cultures on lignin-rich substrates supplemented or not with xylan as a carbon source. Growth on kraft lignin (KL), steam exploded wheat straw (SEWS), and wheat straw (WS) (A-B-C) without (continuous lines) and with added xylan (dotted lines). Enzymatic activities on KL, SEWS and WS alone (D-E-F) and with added xylan (G-H-I). The values are the means ± standard deviations of triplicate cultures.

lignin rich substrates supplemented with xylan cultures, lag phases remained present in contrast to cultures with xylan alone (see See Supplementary Material). Lag phases allow microbial adaptation to the surrounding environment by detoxification or by the production of enzymes necessary for the use of complex substrates as observed in various ligninolytic bacteria grown on aromatic compounds (Aston et al., 2016; Glaser and Venus, 2017). The addition of xylan greatly improved *TX* growth in KL and SEWS cultures. The lag phase duration was shortened in KL cultures. The strong growth on lignin-rich substrates in the presence of additional xylan and the absence of a lag phase in xylan culture showed the negative impact of lignin on *TX* growth.

The dynamics of POX activity remained predominantly intracellular in the presence of xylan-supplemented KL, but the production level was approximately 2 times higher than that in the presence of KL alone at the beginning of growth ($p < 0.001$) (Fig. 1G). Then, POX IC levels decreased drastically over time. POX EC activities were also detected but at very low levels during cultivation (Fig. 1G). One can hypothesize that POX EC are not needed as xylan is present. POX IC enable direct bacterial use of phenolic compounds from KL at the onset of growth and may also detoxify the media. When phenolic molecules are used, POX IC is no longer necessary. This can explain the shorter lag phase and better growth observed on the KL-supplemented media. On xylan-supplemented SEWS, the dynamic production of POX EC or IC was similar to that observed in the presence of SEWS alone (Fig. 1E–H). The levels of POX EC did not significantly change after supplementation, whereas POX IC activities increased after 25 h ($p < 0.05$). Concomitant with the presence of POX IC and EC, xylanase activities were detected in the culture medium in contrast to those in the culture on SEWS alone. Abundant assimilable xylan can help the bacterium use the SEWS complex substrate by producing phenoloxidase. However, as *TX* growth on SEWS was low, one cannot exclude the possibility that inhibitory molecules in SEWS stimulate the production of POX IC to quickly

detoxify the medium and allow bacterial growth on the available xylan.

In xylan supplemented WS cultures, POX activities were reduced significantly ($p < 0.001$) and xylanase activity increased during cultivation. The abundance of xylan in the media, fully available for growth limits the production of unnecessary enzymes such as POX.

3.3. Proteomic approach

3.3.1. General features of the Thermobacillus xylanilyticus proteomes on xylan-supplemented lignin-rich substrates

Approximately 10 % of the 3956 proteins identified were encoded in the *TX* genome (between 375 and 400 different proteins according to the substrate). IC proteins represented 83–87 % of the total detected proteins. Between 48 and 69 proteins were identified as secreted proteins in the EC compartment (presence of a signal peptide). A total of 258 (EC) and 22 (IC) proteins were common to all substrates (including xylan). The IC samples displayed 20, 30, 19 and 13 unique proteins in cultures with xylan, WS, SEWS and KL, respectively, whereas 20, 11, 5 and 19 unique proteins were identified in the EC compartment (data not shown).

The functions of the identified proteins and their abundances are shown in Fig. 2. Most IC proteins are involved in different metabolic pathways, such as sugar metabolism and utilization, amino acid or protein synthesis and ribosomal proteins, and transport proteins (Fig. 2A). Oxidoreductases were the most abundant proteins and represented between 32 and 36 % of the expressed proteins (between 76 and 82 different oxidoreductases). In the EC compartments, proteins with unknown function, transport proteins and hemicellulases were the most abundant. Oxidoreductases represented 5–13 % of all secreted EC proteins depending on the substrate (Fig. 2B).

3.3.2. Hemicellulase expression on xylan-supplemented lignin-rich substrates

Hemicellulases (only 3 % of the IC proteins) were represented by 30 different proteins (Fig. 2A). These enzymes are mainly exo- and debranching enzymes constituted by 7 arabinosidases/xylosidases (several GH43/GH51, including *TX*-Abf51/AbfD3, one GH120 and one GH 127); 1 alpha glucuronidase, GH67; 4 carbohydrate esterases; and 1galactosidase. Three IC xylanases (1 GH8 reducing end exo xylanase and 2 GH10 Txyl_16830 and *Tx*-xyn10, already characterized as Txyl_16210) were also identified. These IC xylanases and the unique glucuronidase GH67 did not significantly differ in expression between any of the substrates, including xylan. Eleven IC hemicellulases expressed on the four substrates were differentially expressed (q value < 0.05) (See Supplementary Material). In the EC compartment, 16 different hemicellulases were identified and represented between 15 and 21 % of all secreted ECs depending on the substrate (Fig. 2B). Eight of these hemicellulases had a signal peptide. Five xylanases (2 GH11 endoxylanases, encoded by the Txyl_04370 and Txyl_04380 genes; Txyl_00055 a multimodular and membrane endoxylanase GH10 and 2 endoxylo-glucanases from the GH9 and GH16 families) represented between 45 and 51 % of all EC hemicellulases depending on the substrates. Among the 8 EC proteins, 6 were differentially expressed under the 4 conditions (q value < 0.05). In the presence of hemicellulose (xylan or complex hemicellulose within lignin-rich substrates), *TX* produced mainly exoenzymes (debranching and accessory hemicellulases) intracellularly and endoenzymes (xylanases) extracellularly, as previously shown (Rakotoarivonina et al., 2014). Moreover, *TX* produces a core set of hemicellulases (xylanases, glucuronidases, and xylosidases/arabinosidases) regardless of the substrate, as similarly reported for other hemicellulolytic bacteria that are able to use aldouronate/methylglucuronoxylan (Chow et al., 2022; De Maayer et al., 2014).

To understand the impact of lignin components on hemicellulase production, the expression levels of hemicellulases on lignin-rich substrates were compared with those on xylan alone (See Supplementary Material). The highest expression of endoenzymes (xylanases and xyloglucanases) was obtained on WS (with overexpression varying up to ~ 8-fold compared to that of xylan). Both GH11 xylanases (*Txyl*_04370 and *Txyl*_04380) were similarly overexpressed. Several esterases were specifically overexpressed (*Txyl*_00800, an acetyl-xylan esterase CE7; *Txyl*_15880, a carboxyl esterase CE10; and *Txyl*_09630, the feruloyl esterase CE1). The feruloyl esterase *Txyl*_09630 was ~ 27-fold and ~ 9-fold higher in the EC and IC, respectively. Feruloyl esterases may cut ester bonds between phenolic acids and the arabinose side of xylan in WS and cross-links with lignin, improving lignocellulosic biomass degradation and the liberation of phenolic compounds (Rakotoarivonina et al., 2014). The esterases in combination with xylanases (highly overexpressed) made the hemicelluloses within the WS more accessible and allowed their use and better bacterial growth. In this configuration, the presence of lignin in WS did not impact the behaviour of *TX*.

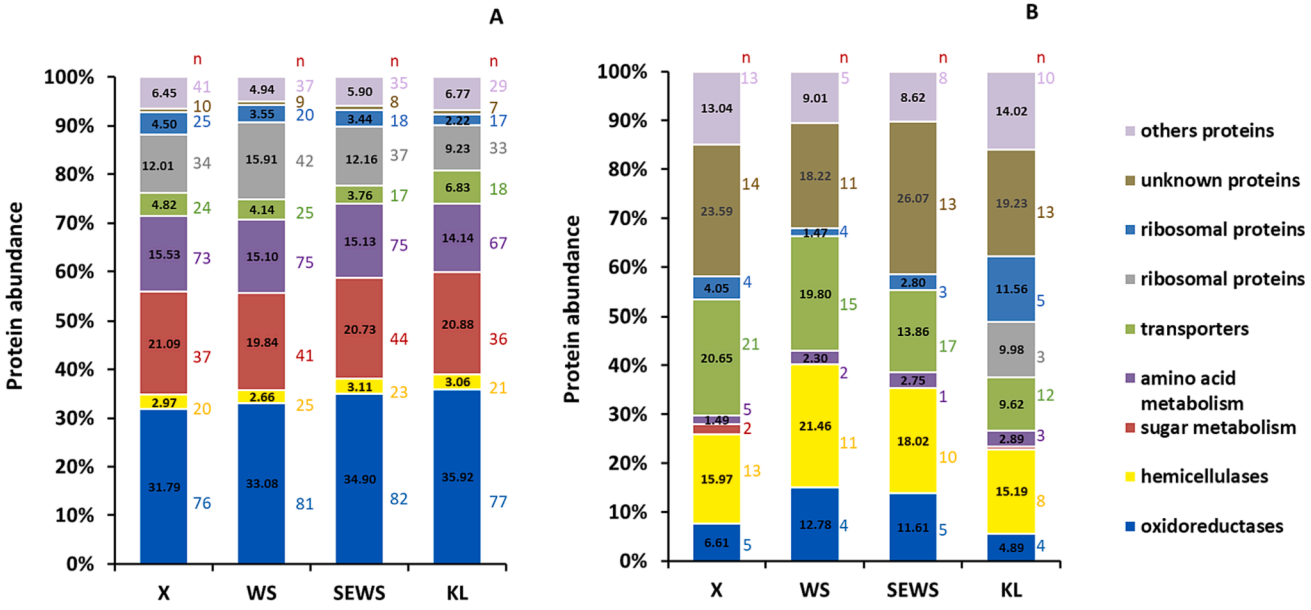

Fig. 2. Functions of the different proteins identified in the intracellular (A) and extracellular (B) proteomes of *TX* cultivated on xylan (X) and on wheat straw (WS), steam exploded wheat straw (SEWS), and kraft lignin (KL). Protein abundance is given in %, and n represents the number of proteins.

On KL, the main result observed was the low expression of EC xylanases produced despite the addition of xylan. Similarly, the expression of the main xylanases GH11 encoded by *Txyl*_04370 and *Txyl*_04380 decreased ~ 4-fold and 1.5-fold, respectively, compared to that under xylan conditions. Even though no xylanase activity was detected in the *TX* culture with KL alone, the xylanase detected in the KL xylan supplemented cultures was stimulated by the addition of xylan. The low production observed may be due either to the inhibitory effect of the lignin itself or even to a possible physical interaction of xylan with lignin, preventing its optimal use by bacteria. IC debranching hemicellulases (arabinofuranosidases/xylosidases, galactosidases, etc.) displayed the highest expression on KL with expression levels between 1.5- and 6-fold higher depending on the enzyme and compared to xylan conditions.) Moreover, the unique glucuronoyl esterase (*Txyl*_12610) exhibited overexpression that was ~ 3-fold higher in KL cultures compared to that in xylan cultures. Like feruloyl esterases, these enzymes are known to cut ester bonds, between glucuronic acid with aromatic rings and linking hemicellulose with lignin. Expression of these proteins facilitates the dissociation of the complex polymer network within lignocellulosic biomasses (Larsbrink and Lo Leggio, 2023; Sainsbury et al., 2013).

For SEWS, the same hemicellulases were expressed with lower levels than in WS cultures but higher than in KL cultures (See Supplementary Material). Additionally, for this substrate, the unique glucuronoyl esterase was also produced by *TX* at the same levels as for KL cultures. Despite the addition of xylan and the higher amount of xylanase (compared to KL, for example), the growth of the bacterium remained low. This difference is probably due to the intrinsic complex structure of the SEWS or the presence of inhibitors, which negatively impact its use, as mentioned above.

Hemicellulases expression and coordination by *TX* depend on the substrates and the presence of lignins within them. The observed specific expression of esterases according to the lignin-rich substrates (KL, SEWS and WS) suggested a tight link between these kinds of hemicellulases and synergy or antagonisms between phenolic compounds, lignins, hemicelluloses and their simultaneous or sequential utilization by the bacterium.

3.3.3. Oxidoreductase expression in xylan supplemented lignin-rich substrates

Proteomic analyses allowed to screen oxidoreductases expressed specifically on the lignin rich substrates. Seventy-four oxidoreductases (61 and 13 IC and EC, respectively) were identified in the different proteomes of *TX* under the four conditions. Twenty of them (18 IC and 2 EC proteins) were differentially expressed with q values < 0.05 (See Supplementary Material). Most of the oxidoreductases had their highest expression levels in KL, SEWS and WS cultures compared with xylan cultures. The overexpression of oxidoreductases has already been reported in recent proteomic studies of ligninolytic bacteria (*B. ligniniphilus* L1, *Pandoraea* sp. ISTKB or *Enterobacter lignolyticus* SCF1) cultivated on lignins (DeAngelis et al., 2013; Kumar et al., 2018; Zhu et al., 2017).

In WS, the expression of oxidoreductase was very low compared to that in KL and SEWS, suggesting that the bacteria do not need to produce these categories of enzymes on this substrate. This finding is in accordance with the low POX activities measured in the media.

The most highly expressed oxidoreductases in the IC compartment on KL were *Txyl*_05820 (Enoyl-[acyl-carrier-protein] reductase [NADH]) and *Txyl*_17475 (encoding the unique catalase/peroxidase present in the genome). These enzymes are implicated in cellular detoxification. Enoyl-[acyl-carrier-protein] reductases [NADH] can degrade phenol groups, while aldo/keto reductases and 3-oxoacyl-[acyl-carrier-protein] reductases can remove carbonyl compounds or furfurals (Huang et al., 2016). In some ligninolytic bacteria grown on KL, peroxidase activities are attributed to the catalase/peroxidase enzymes identified in their genomes and overexpressed (DeAngelis et al., 2013; Falade et al., 2019). Thus, part of the IC POX activity produced by *TX* may be attributed to its various expressed peroxidases and reductases. These observations are in accordance with the predominance of POX IC activity quantified in the presence of KL.

Similarly, in the EC compartment, the overexpression of 8 oxidoreductases was 2- and 4-fold higher on KL compared with that with xylan. These oxidoreductases included peroxidases (*Txyl*_09340 and *Txyl*_11820), ferredoxin (*Txyl*_11890), superoxide dismutase (*Txyl*_05700) and one aryl alcohol dehydrogenase (*Txyl*_03290) also found intracellularly and known for their antioxidant actions which can protect cells from hydrogen peroxide and reactive oxygen species (ROS) accumulation (Kumar et al., 2018; Zhu et al., 2017).

The presence of lignin itself (KL), modified lignin in SEWS or some low-molecular-weight lignin derivatives had an impact on the bacterial utilization of xylan or hemicellulose within lignin-rich substrates (growth). Oxidoreductases implicated in stress response, detoxifications were mainly overexpressed in the *TX* proteomes of KL and SEWS cells intracellularly. One can conclude that the expression of oxidoreductases (mainly IC) associated with high POX activity on these substrates allowed *TX* to overcome this negative impact by detoxifying the culture medium and remove possible inhibitory molecules from lignins.

3.4. Aromatic compounds utilization and oxidoreductases in Thermobacillus xylanilyticus genome

Around 190 oxidoreductases were identified in the genome of *TX* (Rakotoarivonina et al., 2022). These genes were annotated as oxidases (cytochrome *C* oxidases, copper amine oxidases, DPH-dependent quinone oxidoreductase), dehydrogenases/reductases. Five peroxidases and only 2 laccase like / multicopper oxidases which presented homology to characterized laccases from fungi were identified (See Supplementary Materials). No lignin peroxidase (EC 1.11.1.14) was identified within the TX enzyme set. These enzymes are part of lignin-modifying enzymes found in many ligninolytic microorganisms (fungi and bacteria), and their presence can be a marker of ligninolytic activity. Dioxygenases / catechol dioxygenases (14) and monooxygenases (10) were also present in the *TX* genomes. Only few of them presented homology to proteins involved in the intracellular metabolism of aromatic compounds (phenylacetic acid degradation, benzene degradation, and intracellular funneling of aromatics) (See Supplementary Materials). Indeed, no complete pathways concerning the catabolisms of aromatic compound, as in ligninolytic bacteria, were found after analysis. Only eight enzymes (including 2 oxidoreductases TXYL_10380 and TXYL_12405) belonged to benzoate degradation pathways (See Supplementary Materials). This is very low compared to the potential of ligninolytic bacteria (Kumar et al., 2018). Moreover, these enzymes (dioxygenases, laccase like) are not expressed or overexpressed on lignin rich substrates. One can conclude that they could be used occasionally by bacteria to metabolize certain phenolic molecules. This is not surprising as the main characteristic of *TX* is the use of hemicelluloses and lignin or lignin-derived molecules utilizations seem to be a secondary activity for its adaptation to the environment. This can explain the presence and expression of several detoxification enzymes identified by proteomics.

3.5. Characterization of phenolic components in culture media after bacterial growth on xylan-supplemented lignin-rich substrates

For both the controls and the culture media inoculated with *TX*, the phenolic molecules identified by HPLC at the end of incubation were mainly composed of C6-C3 (*p*-coumaric, ferulic and di-ferulic), C6-C1 (*p*-hydroxybenzoic, vanillic, syringic acids), phenolic acids, and C6-C1 aldehydes (*p*-hydroxybenzaldehyde, vanillin, syringaldehyde) (Fig. 3). Vanillic acid was the main phenolic compound released in the KL control media. SEWS control media contained mainly *p*-coumaric acid and vanillin, whereas WS control media contained mainly *p*-coumaric,

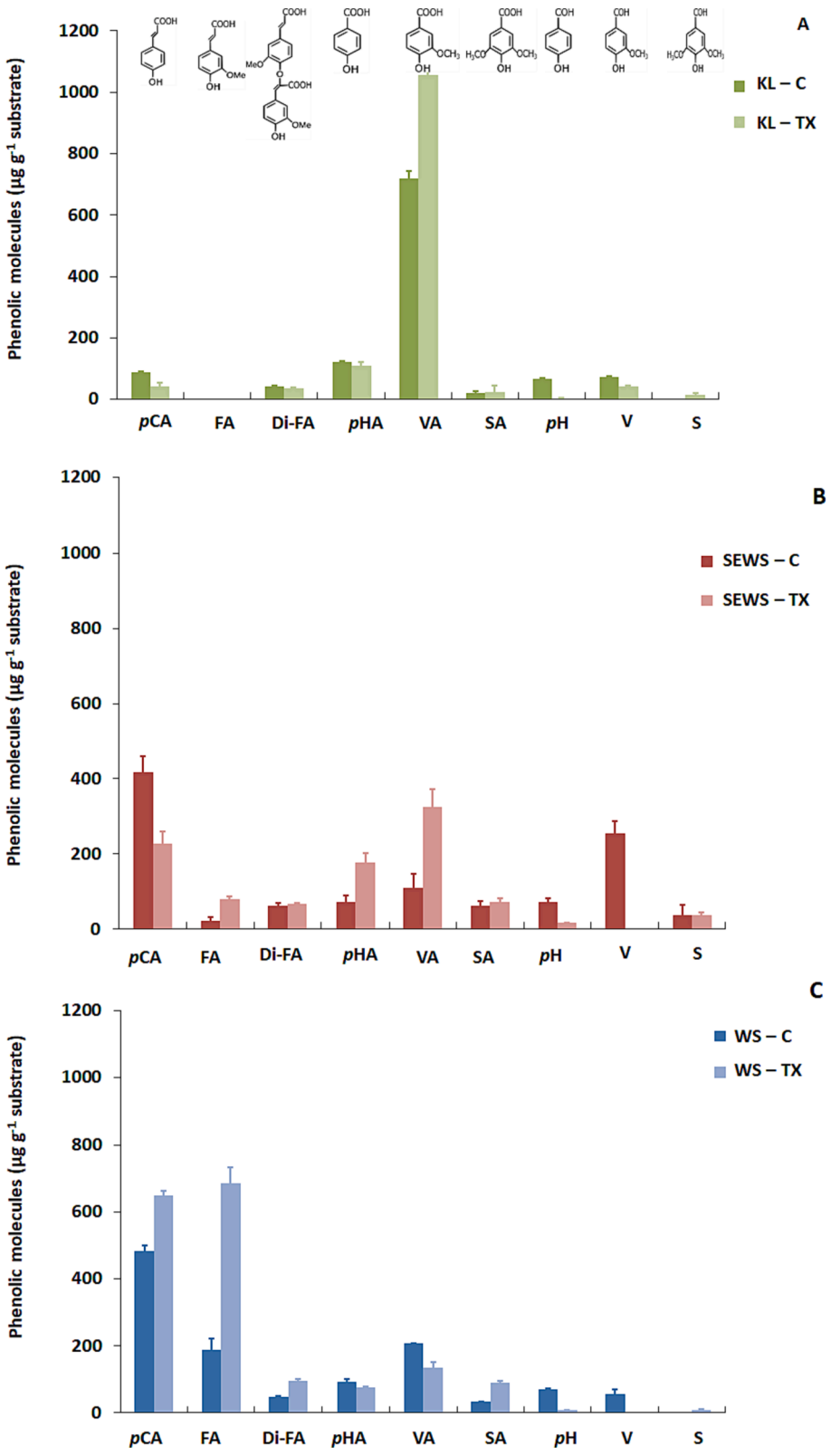

Fig. 3. Contents of phenolic compounds in the culture media after 25 h of incubation in the presence of kraft lignin (A), steam exploded wheat straw (B) and wheat straw (C) without or with *TX* culture supplemented with xylan. *p*-coumaric acid (pCA); ferulic acid (FA); diferulic acid (Di-FA); *p*-hydroxybenzoic acid (*p*HA); vanillic acid (VA); syringic acid (SA); *p*-hydroxybenzaldehyde (*p*H); vanillin (V) and syringaldehyde (S). The values are the means ± standard deviations of triplicate assays.

vanillic and ferulic acids. The occurrence of these compounds in control media may result from a modification of the substrates after autoclaving (Lankiewicz et al., 2023). They could impact directly the microbial behaviour, as these molecules are potential inhibitors of microbial growth (Klinke et al., 2004). They can also be used as carbon sources and may reflect the potential ability of bacteria to use lignin and metabolize its phenolic derivatives (Azubuike et al., 2022). After bacterial growth, the profiles (nature and content) of phenolic compounds varied

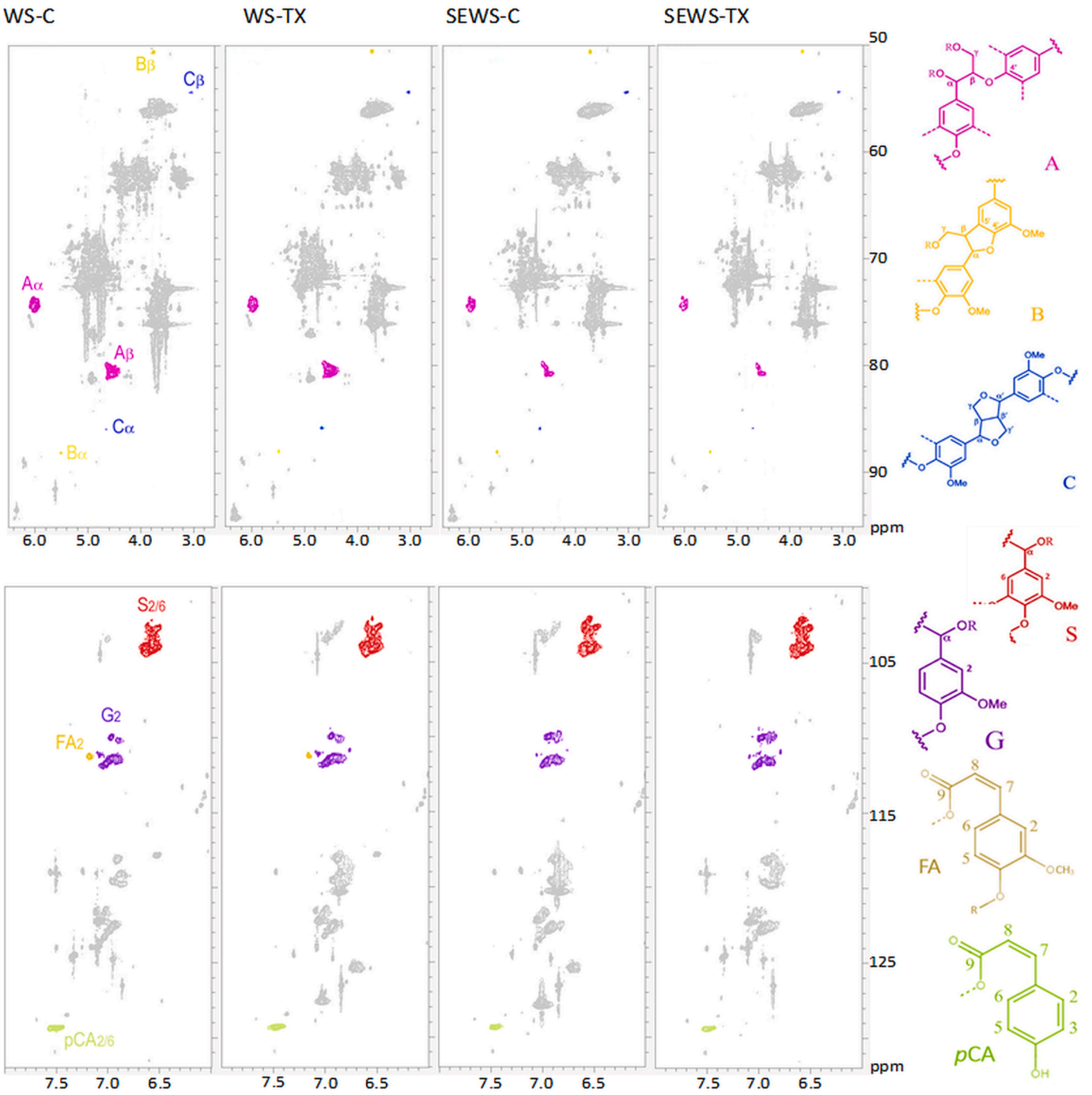

Fig. 4. 2D-NMR analysis of WS and SEWS after 25 h of incubation without (C) or with *TX* culture supplemented with xylan. A, aryl ether bonds (β-O-4); B, phenyl coumaran bonds (β-5); C, resinol bonds (β-β); G, guaiacyl units; S, syringyl units; FA, ferulic acid; *p*CA *p*-coumaric acid.

according to the substrate (Fig. 3). In WS cultures, there was a large increase in the phenolic acid content (4, 1.3, 3 and 2 times, respectively for ferulic, *p*-coumaric, syringic and diferulic acid contents compared to those in the control; p value < 0.001). The proteomic approach showed the expression and overexpression of xylanases (*e.g.*, GH11 *Txyl*_04370) and esterases (*e.g.*, the feruloyl esterase CE1 *Txyl*_09630) by *TX* grown on WS in addition to the core hemicellulases expressed on all substrates. The increased expression of xylanases and esterases may have resulted in increased release of phenolic acids from WS by the enzymatic disruption of ester bonds with hemicelluloses as previously shown (Rakotoarivonina et al., 2014).

In KL and SEWS media with *TX*, the vanillic acid content increased by 3-fold ($p < 0.001$) and 1.5-fold ($p < 0.01$), respectively. This increase was accompanied by significant decreases in vanillin, *p*-hydroxybenzaldehyde and *p*-coumaric acid levels. Similarly, during *B. ligniniphilus* growth on KL, large amount of vanillic acid was quantified whereas vanillin concentration in the culture medium decreases (Zhu et al., 2017). Most phenolic monomers or dimers (biphenyl, phenylcoumaran) are often converted into vanillic acid *via* various pathways before they are transformed into protocatechuates by demethylation (Azubuike et al., 2022). Thus, vanillate decarboxylases are involved in the degradation of biphenyl compounds by decarboxylating 5-carboxyvanillate to vanillic acids after dimer cleavage (Masai et al., 2007). Vanillin is also an intermediary metabolite during the

catabolism of phenolic compounds, and could later be transformed into vanillic acid by vanillate dehydrogenases (vdh) in numerous ligninolytic bacteria. Sainsbury et al. (2013) showed that deletion of the *vdh* gene in the actinobacteria *R. jostii* leads to vanillin and p-hydroxy-benzaldehyde accumulation. The authors also observed the absence of vanillin and p-hydroxybenzaldehyde in fermentation media supplemented with wild-type *R. jostii,* and they demonstrated that vanillin was derived from alkali lignin isolated from wheat straw, probably after the hydrolysis of ferulate ester linkages by esterases. The presence of esterases and glucuronoyl esterase (CE15) in the extracellular *TX* proteomes on KL and SEWS will help the bacterium deconstruct lignin carbohydrate complex (LCC) by cutting ester bonds (Larsbrink and Lo Leggio, 2023) and facilitate the action of oxidoreductases to oxidize lignin and release vanillic acid. On the KL and SEWS proteomes, no decarboxylases were expressed, but several IC dehydrogenases were overexpressed (Txyl_10010, Txyl_16370, Txyl_14210, Txyl_03796, and Txyl_05670) (See supplementary data). Thus, the depletion of vanillin and increase in vanillic acid in *TX* cultures could be due to the transformation of vanillin by these enzymes. However, the exact origin of vanillic acid and other phenolic compounds in *TX* cultures remains to be investigated. This could be either a consequence of direct degradation by the various oxidoreductases identified on lignin or modified lignin-rich substrates or by the intracellular metabolism and conversion of phenolic monomers for detoxification.

3.6. Characterization of lignin-rich residues after bacterial growth on xylan-supplemented lignin-rich substrates

Fourier transform infrared (FTIR) analysis was performed to view changes in the chemical functions of the residues after 25 h of incubation without and with bacterial growth on xylan-supplemented substrates (See Supplementary Material). The WS and KL FTIR spectra showed a large decrease in band intensity between 900 and 1250 cm^{-1}, which corresponds to polysaccharides. These changes may be due to the depletion of hemicelluloses in WS and KL cultures. No significant difference was observed in the spectra of the SEWS residues before and after growth, even in the polysaccharide spectral region. The xylan added was not used by *TX* probably due to its interaction with SEWS components, which physically limits its accessibility. This may explain the lower growth of *TX* on xylan-supplemented SEWS compared to that on WS and KL. The small decrease in the intensity of two bands assigned to lignin (1510 and 1400 cm^{-1}) and the lack of variation in the intensity of aromatic vibration bands of WS and SEWS (1595, 1510, 1460, 1400 cm^{-1}) indicated a weak effect of the bacterium on lignin. It did not provide any precise indication of the extent of possible lignin structural changes.

Therefore, liquid-phase 2D-NMR analysis was performed on WS and SEWS residues without and with bacterial growth in xylan-supplemented cultures (Fig. 4). It allows analysis of the lignin phenolic units, phenolic acids and main interunit linkages, including β-O-4 (A), β-5 (B) and β-β (C) linkages. The main interunit bonds observed are the β-O-4, with small proportions of β-5 and β-β linkages. The S/G ratios (0.6 and 0.7 for WS and SEWS, respectively) did not significantly differ after *TX* growth compared to those of the control, but the proportion of β-O-4 linkages slightly decreased. Thus, β-O-4 linkages represented 80 ± 7 and 70 ± 5 % of the G-units in the control WS and SEWS residues and 78 ± 8 and 63 ± 5 % with *TX* suggesting weak alteration of the lignin structure by the bacterium. Such slight lignin modifications are in accordance with the absence of ligninolytic lignin peroxidase and β etherases in the genome and the different proteomes of *TX*. Supporting the occurrence of degradation by *TX*, the content of phenolic acids decreased after bacterial growth. *p*-Coumaric acid represented11 ± 1 and 7 ± 0 % of the G-units in the control WS and SEWS residues respectively, and 9 ± 1 and 7 ± 0 % after *TX* growth. Ferulic acid, identified by 2D NMR (FA carbon 2), was measured only in WS residues and decreased from 12 ± 1 of the G-units in the control to 8 ± 1 % after *TX* growth. In a recent study, S/G ratios of lignin were modified after the growth of the anaerobic fungus *Neocallimastix californiae* on switchgrass, sorghum and poplar (Lankiewicz et al., 2023). The structural lignin characteristics of WS were shown to be modified after digestion with bacterial consortia from gut termites (decrease in the S:G ratio, tricin, phenolic acid) (Dumond et al., 2021). The results obtained in this study agree with previous data showing only minor structural changes in lignin after the growth of the cellulolytic bacterium *Clostridium thermocellum* on poplar lignocelluloses (Akinosho et al., 2017). Taking these results into account, it is possible that i) POX activities, which are accessory activities produced by *TX*, are not enough efficient to depolymerize lignins within the lignin-rich substrates, ii) unlike fungi, which are known to degrade lignin well, extensive degradation by bacteria likely requires the combination of several microorganisms.

4. Conclusions

This study shows a first insight to the molecular functioning of *T. xylanilyticus* on technical lignins and biorefinery side-products. Substrates with different structures and compositions induced specific physiological response (growth, xylanase and phenoloxidase activities, proteomes). Weak lignin modifications, and significant phenolic productions were evidenced. The overexpressed oxidoreductases, are probably involved in detoxification of phenolic compounds and lignin modifications. For the first time a strict hemicellulolytic bacterium was shown to mobilize concomitantly hemicellulases and phenoloxidases to grow on lignin and lignin-rich substrates. The behavior plasticity of this thermophilic bacterium opens the way for the valorization of broad spectra lignocellulosic substrates.

Funding

The QC PhD was cofunded by the Grand Reims Urban Community and the EU-FEDER Fund in the frame of the Lignofrac project; Operating costs were supported by the Chaire AFERE with funding of Grand Reims Urban Community.

CRediT authorship contribution statement

Quentin Czerwiec: Writing – original draft, Investigation. **Brigitte Chabbert:** Writing – review & editing, Writing – original draft, Formal analysis, Data curation, Conceptualization. **David Crônier:** Investigation. **Bernard Kurek:** Writing – review & editing, Writing – original draft, Conceptualization. **Harivony Rakotoarivonina:** Writing – review & editing, Writing – original draft, Validation, Supervision, Project administration, Funding acquisition, Formal analysis, Data curation, Conceptualization.

Declaration of competing interest

The authors declare that they have no known competing financial interests or personal relationships that could have appeared to influence the work reported in this paper.

Data availability

Data will be made available on request.

Acknowledgements

The authors thank Corinne Ivaldi for her help in preparing the proteomic samples; Anouck Habrant for infrared analysis; Veronique Aguié-Béghin for discussions on lignins; ARD (France) for providing WS; and IFPEN, France for SEWS, which was produced in the frame of the ANR project Funlock (ANR-13-BIME-0002).

Appendix A. Supplementary data

Supplementary data to this article can be found online at https://doi.org/10.1016/j.biortech.2024.130507.

References

Abdelaziz, O.Y., Hulteberg, C.P., 2017. Physicochemical characterisation of technical lignins for their potential valorisation. Waste Biomass Valoriz. 8 (3), 859–869.

Akinosho, H.O., Yoo, C.G., Dumitrache, A., Natzke, J., Muchero, W., Brown, S.D., Ragauskas, A.J., 2017. Elucidating the structural changes to populus lignin during consolidated bioprocessing with *Clostridium thermocellum*. ACS Sustain. Chem. Eng. 5 (9), 7486–7491.

Aston, J.E., Apel, W.A., Lee, B.D., Thompson, D.N., Lacey, J.A., Newby, D.T., Reed, D.W., Thompson, V.S., 2016. Degradation of phenolic compounds by the lignocellulose deconstructing thermoacidophilic bacterium *Alicyclobacillus acidocaldarius*. J. Ind. Microbiol. Biotechnol. 43 (1), 13–23.

Auxenfans, T., Cronier, D., Chabbert, B., Paes, G., 2017. Understanding the structural and chemical changes of plant biomass following steam explosion pretreatment. Biotechnol. Biofuels 10.

Azubuike, C.C., Allemann, M.N., Michener, J.K., 2022. Microbial assimilation of lignin-derived aromatic compounds and conversion to value-added products. Curr. Opin. Microbiol. 65, 64–72.

Ballesteros, I., Negro, M.J., Oliva, J.M., Cabanas, A., Manzanares, P., Ballesteros, M., 2006. Ethanol production from steam-explosion pretreated wheat straw. Appl. Biochem. Biotechnol. 130 (1–3), 496–508.

Bugg, T.D.H., Williamson, J.J., Rashid, G.M.M., 2020. Bacterial enzymes for lignin depolymerisation: new biocatalysts for generation of renewable chemicals from biomass. Curr. Opin. Chem. Biol. 55, 26–33.

Chow, V., Nong, G., St John, F.J., Sawhney, N., Rice, J.D., Preston, J.F., 2022. Bacterial xylan utilization regulons: systems for coupling depolymerization of methylglucuronoxylans with assimilation and metabolism. J. Ind. Microbiol. Biotechnol. 49 (2).

da Silva Vilar, D., Bilal, M., Bharagava, R.N., Kumar, A., Kumar Nadda, A., Salazar-Banda, G.R., Eguiluz, K.I.B., Romanholo Ferreira, L.F., 2022. Lignin-modifying enzymes: a green and environmental responsive technology for organic compound degradation. J. Chem. Technol. Biotechnol. 97 (2), 327–342.

De Maayer, P., Brumm, P.J., Mead, D.A., Cowan, D.A., 2014. Comparative analysis of the *geobacillus* hemicellulose utilization locus reveals a highly variable target for improved hemicellulolysis. BMC Genom. 15.

DeAngelis, K.M., Sharma, D., Varney, R., Simmons, B., Isern, N.G., Markilllie, L.M., Nicora, C., Norbeck, A.D., Taylor, R.C., Aldrich, J.T., Robinson, E.W., 2013. Evidence supporting dissimilatory and assimilatory lignin degradation in *Enterobacter lignolyticus* SCF1. Frontiers in Microbiology, p. 4.

Dumond, L., Lam, P.Y., van Erven, G., Kabel, M., Mounet, F., Grima-Pettenati, J., Tobimatsu, Y., Hernandez-Raquet, G., 2021. Termite gut microbiota contribution to wheat straw delignification in anaerobic bioreactors. ACS Sustain. Chem. Eng. 9 (5), 2191–2202.

Falade, A.O., Mabinya, L.V., Okoh, A.I., Nwodo, U.U., 2019. Studies on peroxidase production and detection of sporotrichum thermophile-like catalase-peroxidase gene in a *Bacillus* species isolated from hogsback forest reserve, South Africa. Heliyon 5 (12).

Glaser, R., Venus, J., 2017. Model-based characterisation of growth performance and L-lactic acid production with high optical purity by thermophilic *Bacillus coagulans* in a lignin-supplemented mixed substrate medium. N. Biotechnol. 37, 180–193.

Huang, Y.H., Lin, J.S., Ma, J.C., Wang, H.H., 2016. Functional characterization of triclosan-resistant enoyl-acyl-carrier protein reductase (FabV) in *Pseudomonas aeruginosa*. Front. Microbiol. 7.

Iiyama K, W.A.F.A., 1988. An improved acetyl bromide procedure for determining lignin in woods and wood pulps. Wood Sci. Technol. 22 (September), 271–280.

Ishihama, Y., Oda, Y., Tabata, T., Sato, T., Nagasu, T., Rappsilber, J., Mann, M., 2005. Exponentially modified protein abundance index (emPAI) for estimation of absolute protein amount in proteomics by the number of sequenced peptides per protein. Mol. Cell. Proteomics 4 (9), 1265–1272.

Klinke, H.B., Thomsen, A.B., Ahring, B.K., 2004. Inhibition of ethanol-producing yeast and bacteria by degradation products produced during pre-treatment of biomass. Appl. Microbiol. Biotechnol. 66 (1), 10–26.

Kumar, M., Verma, S., Gazara, R.K., Kumar, M., Pandey, A., Verma, P.K., Thakur, I.S., 2018. Genomic and proteomic analysis of lignin degrading and polyhydroxyalkanoate accumulating beta-proteobacterium *pandoraea* sp ISTKB. Biotechnol. Biofuels 11.

Lankiewicz, T.S., Choudhary, H., Gao, Y., Amer, B., Lillington, S.P., Leggieri, P.A., Brown, J.L., Swift, C.L., Lipzen, A., Na, H.Y.S., Amirebrahimi, M., Theodorou, M.K., Baidoo, E.E.K., Barry, K., Grigoriev, I.V., Timokhin, V.I., Gladden, J., Singh, S., Mortimer, J.C., Ralph, J., Simmons, B.A., Singer, S.W., O'Malley, M.A., 2023. Lignin deconstruction by anaerobic fungi. Nat. Microbiol. 8 (4), 596-+.

Larsbrink, J., Lo Leggio, L., 2023. Glucuronoyl esterases-enzymes to decouple lignin and carbohydrates and enable better utilization of renewable plant biomass. Essays Biochem. 67 (3), 493–503.

Mansfield, S.D., Kim, H., Lu, F.C., Ralph, J., 2012. Whole plant cell wall characterization using solution-state 2D NMR. Nat. Protoc. 7 (9), 1579–1589.

Mardetko, N., Trontel, A., Novak, M., Pavlecic, M., Ljubas, B.D., Grubisic, M., Tominac, V.P., Ludwig, R., Santek, B., 2021. Screening of lignocellulolytic enzyme activities in fungal species and sequential solid-state and submerged cultivation for the production of enzyme cocktails. Polymers 13 (21).

Masai, E., Katayama, Y., Fukuda, M., 2007. Genetic and biochemical investigations on bacterial catabolic pathways for lignin-derived aromatic compounds. Biosci. Biotech. Bioch. 71 (1), 1–15.

McCann, M.C., Carpita, N.C., 2015. Biomass recalcitrance: a multi-scale, multi-factor, and conversion-specific property. J. Exp. Bot. 66 (14), 4109–4118.

Mesle, M.M., Mueller, R.C., Peach, J., Eilers, B., Tripet, B.P., Bothner, B., Copie, V., Peyton, B.M., 2022. Isolation and Characterization of Lignocellulose-Degrading *Geobacillus thermoleovorans* from Yellowstone National Park (vol 88, e00958-21, 2022). Appl. Environ. Microbiol., 88(9).

Moretti, C., Corona, B., Hoefnagels, R., Vural-Gürsel, I., Gosselink, R., Junginger, M., 2021. Review of life cycle assessments of lignin and derived products: Lessons learned. Sci. Total Environ., 770.

Nargotra, P., Sharma, V., Lee, Y.C., Tsai, Y.H., Liu, Y.C., Shieh, C.J., Tsai, M.L., Dong, C. D., Kuo, C.H., 2023. Microbial lignocellulolytic enzymes for the effective valorization of lignocellulosic biomass: a review. Catalysts 13 (1), 28.

Rakotoarivonina, H., Hermant, B., Aubry, N., Rabenoelina, F., Baillieul, F., Remond, C., 2014. Dynamic study of how the bacterial breakdown of plant cell walls allows the reconstitution of efficient hemicellulasic cocktails. Bioresour. Technol. 170, 331–341.

Rakotoarivonina, H., Loux, V., Doliwa, C., Martin, V., Remond, C., 2022. Draft genome sequence of the lignocellulolytic and thermophilic bacterium *Thermobacillus xylanilyticus* XE. Microbiol. Resour. Announcements 11 (4).

Ralph, J., 2010. Hydroxycinnamates in lignification. Phytochem. Rev. 9 (1), 65–83.

Ravi, K., Abdelaziz, O.Y., Nobel, M., Garcia-Hidalgo, J., Gorwa-Grauslund, M.F., Hulteberg, C.P., Liden, G., 2019. Bacterial conversion of depolymerized Kraft lignin. Biotechnol. Biofuels 12.

Sainsbury, P.D., Hardiman, E.M., Ahmad, M., Otani, H., Seghezzi, N., Eltis, L.D., Bugg, T. D.H., 2013. Breaking down lignin to high-value chemicals: the conversion of lignocellulose to vanillin in a gene deletion mutant of *Rhodococcus jostii* RHA1. ACS Chem. Biol. 8 (10), 2151–2156.

Scheller, H.V., Ulvskov, P., 2010. Hemicelluloses. In: Annual Review of Plant Biology, Vol 61, (Eds.) S. Merchant, W.R. Briggs, D. Ort, Vol. 61, pp. 263-289.

Sethupathy, S., Morales, G.M., Gao, L., Wang, H., Yang, B., Jiang, J., Sun, J., Zhu, D., 2022. Lignin valorization: status, challenges and opportunities. Bioresour. Technol. 347.

Shi, Q.C., Li, Y.Q., Li, Y.F., Cheng, Y., Zhu, W., 2019. Effects of steam explosion on lignocellulosic degradation of, and methane production from, corn Stover by a co-cultured anaerobic fungus and methanogen. Bioresour. Technol. 290.

Taylor, C.R., Hardiman, E.M., Ahmad, M., Sainsbury, P.D., Norris, P.R., Bugg, T.D.H., 2012. Isolation of bacterial strains able to metabolize lignin from screening of environmental samples. J. Appl. Microbiol. 113 (3), 521–530.

Zhang, W., Diao, C.Y., Wang, L., 2023. Degradation of lignin in different lignocellulosic biomass by steam explosion combined with microbial consortium treatment. Biotechnol. Biofuels Bioprod. 16 (1).

Zhu, D.C., Zhang, P.P., Xie, C.X., Zhang, W.M., Sun, J.Z., Qian, W.J., Yang, B., 2017. Biodegradation of alkaline lignin by *Bacillus ligniniphilus* L1. Biotechnol. Biofuels 10.